Materials and Design 31 (2010) 336–342

Contents lists available at ScienceDirect

Materials and Design

journal homepage: www.elsevier.com/locate/matdes

# Assessment of the effect of existing corrosion on the tensile behaviour of magnesium alloy AZ31 using neural networks

V. Kappatos *, A.N. Chamos, Sp.G. Pantelakis

*Laboratory of Technology and Strength of Materials, Department of Mechanical Engineering and Aeronautics, University of Patras, Panepistimoupolis Rio, 26500 Patras, Greece*

ARTICLE INFO

*Article history:*
Received 18 May 2009
Accepted 8 June 2009
Available online 10 June 2009

*Keywords:*
Magnesium alloy
Mechanical properties
Corrosion damage
Neural networks

ABSTRACT

A concept has been devised to assess the effect of existing corrosion damage on the residual tensile properties of structural alloys and applied for the magnesium alloy AZ31. The concept based on the use of a radial basis function neural network. An extensive experimental investigation, including metallographic corrosion characterization and mechanical testing of pre-corroded AZ31 magnesium alloy specimens, was carried out to derive the necessary data for the training and the prediction module of the developed neural network model. The proposed concept was exploited to successfully predict: the gradual tensile property degradation of the alloy AZ31 to the results of gradually increasing corrosion damage with increasing corrosion exposure.



## 1. Introduction

The multifarious variables that are involved in corrosion of structures in-service are convoluted, complex and interacting [1]. On the other hand, traditional approaches to understanding and assessing the effects of corrosion on structural components rely on classic textbooks models of general corrosion and the metallographic characterization of corrosion damage.

In recent years, a number of incidents (e.g. Aloha, 1988) and the results of various investigations, e.g. [2], provided evidence that the assessment of the effects of corrosion damage on residual strength and integrity of structural components operating in corrosive environment is a problem far more complex than anticipated [1–4].

The development of methodologies capable of facing the above problem requires a comprehensive understanding and characterization of corrosion damage mechanisms and relies heavily on the existence of sufficient experimental data. However, limited experimental data exist in published literature on the mechanical performance of corrosion damaged structural alloys. Examples of such data, mostly obtained from materials subjected to accelerated laboratory corrosion conditions and only very rarely from materials corroded in service may be found, e.g. in [3–10]. Essential cause for the limited amount of such data available is that their production is time consuming and expensive.

The use of Neural Networks (NN) to make predictions of the mechanical properties of alloys is a relatively new concept, but one that has received considerable interest in recent years [11–17]. In [11], the authors have introduced three different back-propagation NN models which can predict the (i) impact toughness of quenched and tempered steels exposed to various postweld heat treatment cycles, (ii) simulated heat affected zone toughness of pipeline steels resulting from in-service welding and (iii) hot ductility and hot tensile strength of microalloyed steels. In [12], some results of the research connected with the development of a new approach based on artificial intelligence for predicting the volume fraction and mean size of the phase constituents occurring in steel after thermomechanical processing and cooling are presented. A NN model was used to predict mechanical properties of dual phase steels and sensitivity analysis was performed to investigate the importance of the effects of pre-strain, deformation temperature, volume fraction and morphology of martensite on room temperature mechanical behaviour of these steels [13].

In [14], a NN was developed for the analysis and simulation of the correlation between the properties of maraging steels and composition, processing and working conditions. The input parameters of the model consist of alloy composition, processing parameters (including cold deformation degree, ageing temperature and ageing time), and working temperature. The outputs of the NN model include property parameters, namely: ultimate tensile strength, yield strength, elongation, reduction in area, hardness, notched tensile strength, Charpy impact energy, fracture toughness and martensitic transformation start temperature.

In [15], a model for predicting the mechanical properties of the alumina matrix ceramic was established by means of a NN, using

* Corresponding author.
*E-mail addresses:* kappatos@mech.upatras.gr (V. Kappatos), hamosa@mech.upatras.gr (A.N. Chamos), pantelak@mech.upatras.gr (Sp.G. Pantelakis).

0261-3069/$ - see front matter © 2009 Elsevier Ltd. All rights reserved.
doi:10.1016/j.matdes.2009.06.009

hardness, elastic modulus, density, as well as content of the matrix material and additives, as the input parameters of the network model. The output parameters of the NN are flexural strength and fracture toughness of the composite ceramic materials. In [16], a model was developed for the analysis and prediction of the correlation between processing (heat treatment) parameters and mechanical properties in titanium alloy by applying NN.

A NN was trained and used to predict fatigue life for specified sets of loading and environmental conditions, using a data base of 1036 fatigue tests for carbon and low-alloy steels in [17]. It covers an adequate range of compositional and structural parameters, loading strain rate, temperature, and water chemistry. By finding patterns and trends in the data, the NN can estimate the fatigue life for any set of conditions.

In the present work, a concept to assess the effect of existing corrosion damage on the tensile behaviour of the wrought magnesium alloy AZ31 has been devised. The concept relies on the exploitation of Radial Basis Function (RBF)-NN. For the developing of the NN, extensive experimental investigation has been carried out including corrosion characterization and measurements of mechanical properties degradation after several corrosion exposure times.

To characterize corrosion average and maximum pit depth as well as pitting density were measured. In the proposed model, these characteristics are used as input parameters in a NN, in order to correlate the corrosion damage to the tensile properties of the corroded material. The developed NN was used for predicting the time dependency of the tensile mechanical properties degradation on the basis of corrosion damage characteristics.

## 2. Experimental work

### 2.1. Material

The experimental investigation was carried out for the magnesium structural alloy AZ31. It was received in sheet from of 2 mm nominal thickness. The material is characterized as high-purity (hp), as the concentration of the contaminants (Fe, Ni and Cu) was held under certain limits. After the rolling procedure the material was subjected to annealing (O-temper) at 300 °C for 30 min. The chemical composition of the alloy is shown in Table 1.

### 2.2. Corrosion tests

To characterize corrosion damage and derive the necessary input data for the NN a number of metallography specimens were exposed to salt spray fog for different exposure times. The exposure times selected for the corrosion tests were 0.5, 3, 6, 12, 24, 48 and 72 h. For the tests rectangular metallography specimens having 100 mm × 50 mm dimensions were cut from the longitudinal direction of the AZ31 sheet. Corrosion damage was predicted by calculating maximum, average and standard deviation of pit depth, average and standard deviation of pitting density, geometrical configuration of the pits in terms of their aspect ratio as well as pitting factor as the ratio of maximum to average pit depth.

### 2.3. Tensile tests

For deriving data to train the NN, a series of tensile tests was carried out following to the exposure of AZ31 tensile specimens to salt spray fog for different exposure times. The tensile tests were machined in longitudinal direction according to the ASTM E8 M specification with 50 mm gauge length and 12.5 mm gauge width at the reduced cross-section. For the tests servo hydraulic MTS 250 KN machine was used for the tensile tests. The tests were carried out according to ASTM E8 M with a constant elongation rate of 2 mm/min. A data logger was used to store the data in a digital file.

Evaluated have been the properties: yield strength ($R_p$) (0.2% proof stress), tensile strength ($R_m$), elongation to fracture ($A_f$), and strain energy density ($W$) (tensile toughness). In the present work, strain energy density has been calculated as the integral of the engineering tensile stress–strain curves up to elongation to fracture. Involving engineering stress–strain curves instead of true stress–true strain curves for calculating $W$ is justified as the observed tensile necking at the elongation to fracture has not been appreciable.

**Table 1**
Chemical composition of magnesium alloy AZ31.

| | Al | Zn | Mn | Fe | Ni | Cu | Mg |
|---|---|---|---|---|---|---|---|
| AZ31 | 3.06 | 0.80 | 0.25 | 0.003 | <0.001 | 0.001 | Bal. |

### 2.4. Corrosion testing procedure

Prior to the corrosion exposure, the surface of the specimens were chemically cleaned in order to remove any oily lubricant, left from the rolling process of the material. Two subsequent solutions were used. The first treatment was immersion of the test specimens for 1 min to a solution contained 10% $HNO_3$ and ethanol. Then the test specimens were immediately immersed for another minute in a solution containing 10% NaOH and 90% distilled water. Afterwards the test specimens were dried and immediately inserted to the corrosive environment.

For the corrosion tests, the accelerated salt spray fog environment has been used. The salt spray tests were conducted according to ASTM B117 specification. The corrosive solution was prepared by dissolving five parts by mass of sodium chloride in 95 parts of distilled water. The pH of the salt solution was such that when atomized at 35 °C the collected solution was in the pH range from 6.5 to 7.2. The pH measurement was made at 25 °C. The temperature at the exposure zone of the salt spray chamber was maintained at 35 ± 1 °C. After the exposure the specimens were cleaned according to ASTM G1 specification. The solution used contained 200 g chromium trioxide ($CrO_3$), 10 g silver nitrate ($AgNO_3$), 20 g barium nitrate ($Ba(NO_3)_2$) and reagent water to make 1000 mL. The pre-corroded tensile specimens were immersed in the above solution for about 1 min to remove the corrosion products from their surface and then immediately dried.

## 3. Experimental results

### 3.1. Corrosion damage characterization

Representative cross-sections of the metallography specimens after different exposure times in the salt spray environment can be seen in Fig. 1. At short exposure times prevailing mechanism is the development of wide and shallow pits as it can be seen for the example of the 3 h corrosion exposure in Fig. 1a,b. For 24 h corrosion exposure time, some wide and shallow pits are still present (Fig. 1c) yet narrow and deep pits are mostly observed (Fig. 1d).

A light microscope Leica DM LM had been used to measure the average and maximum pit depth of the metallography specimens for the investigated exposure times. The average value of the pit depth was determined by the average of 30 pit depth measurements in each metallography specimen. The surface of each plate was divided into sections of 100 $mm^2$ in order to measure the pitting density and to calculate the pitting factor. The pits depth and density were measured and classified according to the standard ASTM G46.

The dependency of pitting density and pit depth on the investigated corrosion exposure times can be seen in the graphs of Fig. 2.

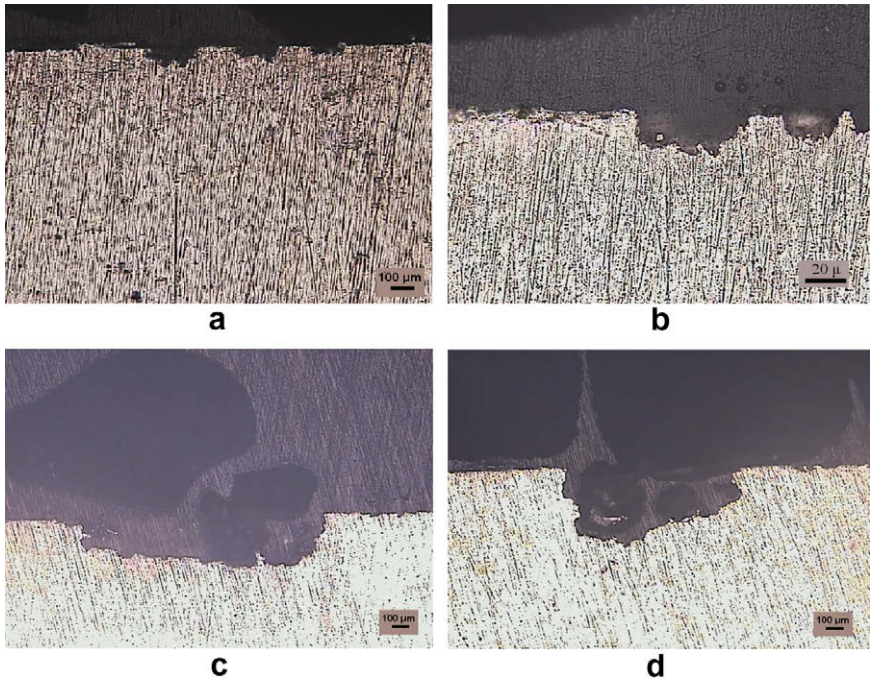


**Fig. 1.** Metallography cross-sections of the pits after salt spray corrosion exposure for (a, b) 3 h and (c, d) 24 h.

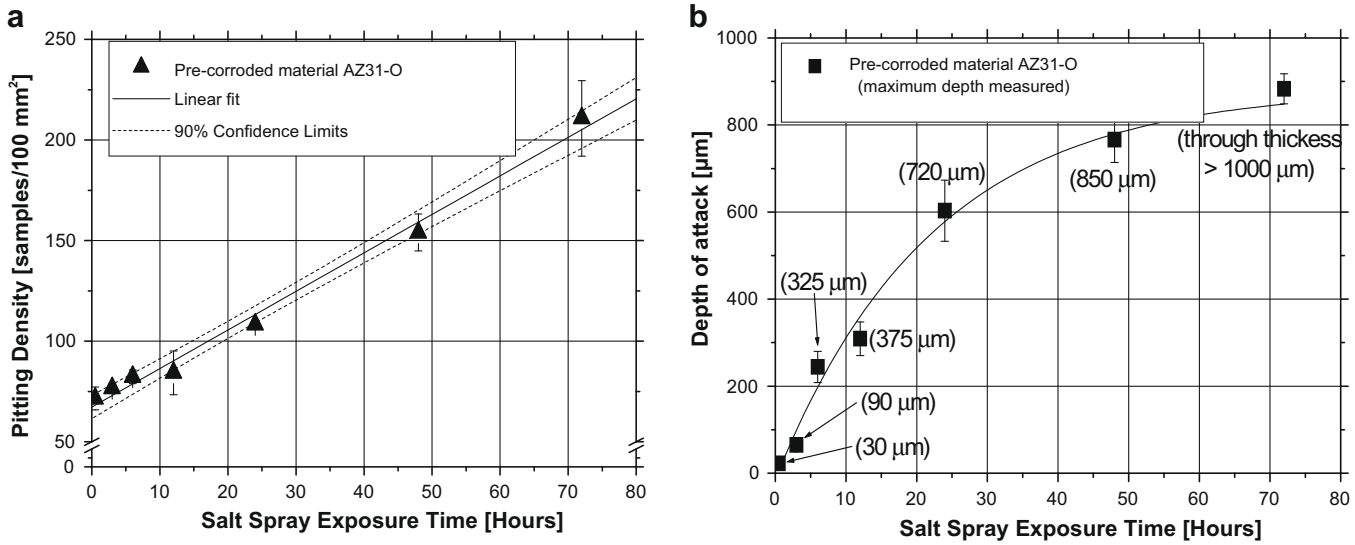


**Fig. 2.** Pitting density and pit depth of attack measurements of the pre-corroded specimens of AZ31-O material.

The pitting density increases almost linearly with increasing corrosion salt spray exposure time (Fig. 2a). The average depth of corrosion attack (pit depth), as well as the maximum pit depth are displayed in Fig. 2b, as a function of the investigated corrosion exposure times. The pit depth seems to increase exponentially with increasing corrosion exposure time. It should be mentioned that for the case of 72 h exposure time, through thickness holes could be seen (nominal thickness of the material = 2.0 mm).

The values of pitting density and pit depth measurements can be also found in Table 2. The pitting factor has been calculated according to the ASTM G46 as the ratio of maximum to average pit depth. As pointed out by the calculated values of the pitting factor, the degradation mechanism seems to change when the corrosion exposure time becomes higher than 6 h. For short exposure times (up to 6 h), the pitting factor takes values of higher than 1.3, while for higher exposure times it seems to decrease and reaches values of about 1.1.

### 3.2. Residual tensile properties

The decrease in tensile strength properties with increasing corrosion exposure time can be seen in Fig. 3a. With increasing corrosion exposure time, a continuous, almost linear decrease in the ultimate tensile strength was observed; it decreases to a value of 170 MPa for an exposure time of 72 h. This corresponds to a 38% reduction as compared to the UTS value of the un-corroded material. The corrosion exposure seems to have a smaller effect on the yield strength of the *L* direction. By an exposure of 72 h it gives a yield strength reduction of 22%. On the other side, a dramatic reduction in tensile ductility has been observed (Fig. 3b), even after

**Table 2**
Pitting prediction according to ASTM G46 on the pre-corroded AZ31-O material.

| Corrosion exposure | Depth of attack (μm) | | | Pitting factor (–) | Pitting density (samples/100 mm$^2$) | |
|---|---|---|---|---|---|---|
| | Average | St. dev. | Maximum | | Average | St. dev. |
| Salt spray corrosion 0.5 h | 22.5 | 5.01 | 30 | 1.33 | 71.50 | 5.68 |
| Salt spray corrosion 03 h | 65.1 | 15.24 | 90 | 1.38 | 76.62 | 2.43 |
| Salt spray corrosion 06 h | 244.3 | 35.86 | 325 | 1.33 | 82.13 | 3.34 |
| Salt spray corrosion 12 h | 309.1 | 38.72 | 375 | 1.21 | 84.25 | 10.85 |
| Salt spray corrosion 24 h | 603.2 | 70.19 | 720 | 1.19 | 108.31 | 2.17 |
| Salt spray corrosion 48 h | 766.2 | 52.19 | 850 | 1.11 | 154.12 | 9.17 |
| Salt spray corrosion 72 h | 883.1 | 34.27 | 1000 | 1.13 | 210.72 | 18.75 |

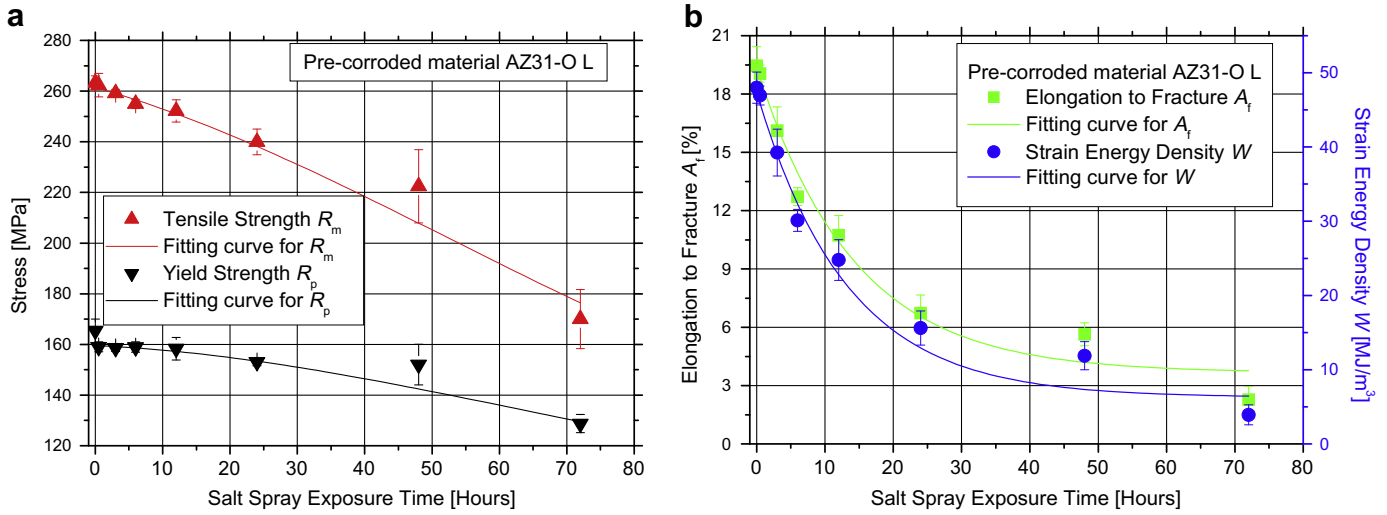


**Fig. 3.** (a) Yield and tensile strength and (b) elongation and strain energy density of AZ31-O alloy in *L* direction after exposure in salt spray environment.

short corrosion exposure times. The decrease of elongation to fracture and energy density is of the order of 35% and 38%, respectively, for 6 h exposure time and reaches the dramatic decrease of 90% and 92%, respectively, at 72 h exposure time.

An overview of the decrease of the tensile properties with increasing exposure time is graphically depicted in Fig. 4.

Fractographic analysis of the tensile specimens has shown the absence of dimples on the fracture surfaces, leading to the conclusion that the fracture mode is quasi-cleavage. As it may be seen from the SEM images in Fig. 5a–d pits develop progressively from the surface of the material with increasing corrosion exposure time. Open and shallow pits were observed after 6 h of corrosion exposure (Fig. 5a), while pits become deeper for the cases of 24 and 48 h of corrosion exposure (Fig. 5b and c). After 72 h of corrosion exposure (Fig. 5d) a crater has been created. It is evident that corrosion has proceeded almost through the thickness of the specimen. The observed crater on the fracture surface served as a notch, leading to fracture of the specimen.

The above observations, combined with the results of the mechanical tests confirm that the decrease of the mechanical properties of the alloy under investigation, and especially of the elongation to fracture, may be attributed to the progressive pit development which acts as corrosion notches. The corrosion notches reduce the ability of the material to accumulate large amounts of plastic deformation. Therefore, the impact of pit depth on the decrease of the mechanical properties is stronger than that of pitting density.

## 4. Neural network model development

The RBF-NN is used to build a system for the prediction of the mechanical properties of the corroded material. RBF-NN can model any nonlinear function using a single hidden layer, which eliminates considerations of determining the number of hidden layers and nodes. The simple linear transformation in the output layer can be optimized fully by using conventional linear modelling techniques, which are fast and less susceptible to the local minima problem. The number of hidden nodes and function parameters of RBF network can be preset in accordance with the prior understanding of the training data or requirements of the output [19]. Not surprisingly, RBF networks are becoming increasingly popular in many scientific areas.

NN modelling usually includes the following steps: (i) data collection; (ii) definition of input/output parameters; (iii) analysis and

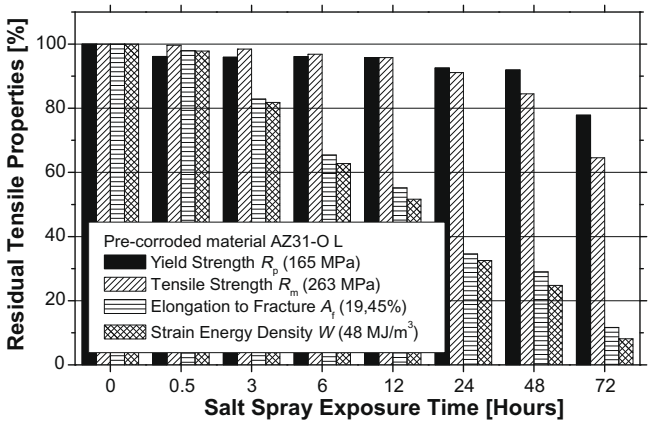


**Fig. 4.** Residual tensile mechanical properties of the AZ31-O alloy after exposure in salt spray environment.

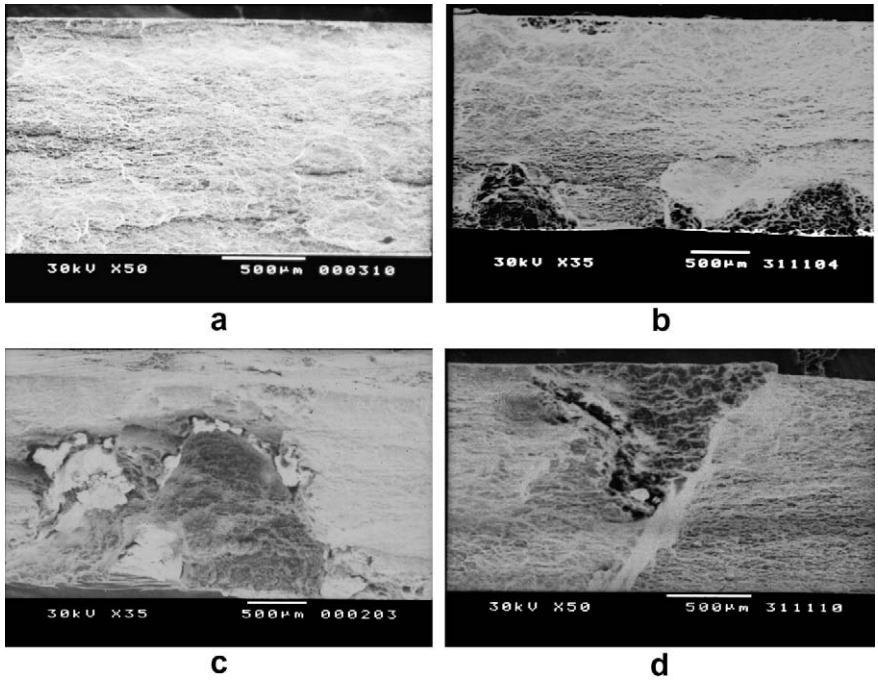


**Fig. 5.** Fracture characteristics of tensile specimens after (a) 6 h, (b) 24 h, (c) 48 h and (d) 72 h exposure in salt spray environment [18].

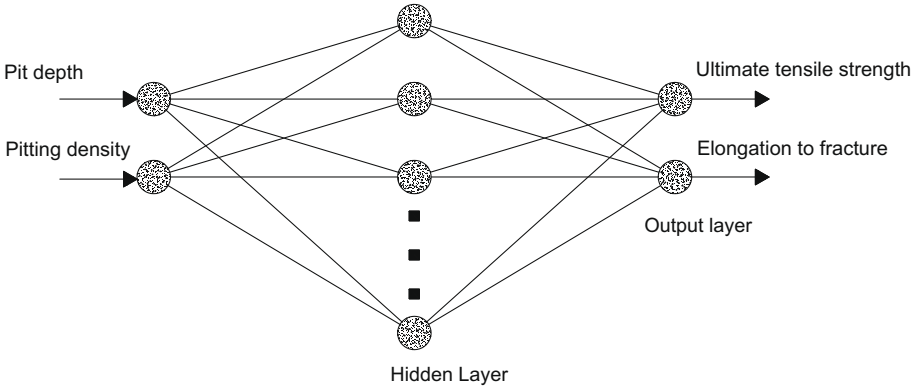


**Fig. 6.** The structure of RBF-NN for prediction of the mechanical properties.

pre-processing of the data; (iv) training of the NN; (v) testing of the trained NN; and (vi) using the trained network for evaluation and prediction.

In order to develop an adequate database for the training and the prediction module, the procedure which was described in the Section 2 was followed.

The definition of the input parameters is a very important aspect of NN modelling. The processing of many parameters not only leads to more computational overhead but often increases enormously the required size of the training data, thereby degrading the classifier performance. The choice should be based on the physical background of a process. In the present work, the input vector consists of two parameters, namely: average pit depth and pitting density which have stronger discriminant capability than the others parameters. As the outputs of the NN, ultimate tensile strength and elongation to fracture were selected. In Fig. 6, the structure of the RBF-NN which is used for prediction of the mechanical properties is displayed.

The prediction module can be more efficient if certain pre-processing algorithms are performed on the training data, i.e. all network inputs are scaled applying a parameter normalization using the mean and the standard deviation of the training set. Thus, the input data were linearly normalized to obtain zero mean and unity standard deviation. The new parameters ensure zero mean and unity standard deviation.

The prediction accuracy is significantly affected by the training method. Model training includes the choice of architecture, training algorithms and parameters of the network. The RBF synaptic weights were estimated using the training procedure described in [19].

For this study, in total 134 input/output data pairs for magnesium alloy AZ31 at different time of corrosion exposure have been used. After network training, where 114 randomly selected pairs were used, the remaining 20 pairs, uniformly distributed in seven exposure corrosion times, were used to evaluate the RBF-NN. The training and the prediction module are repeated for a pre-defined number of iterations, selecting randomly pairs for the prediction phase.

## 5. Neural network results and discussion

The RBF-NN configuration and the selection of the training data are affecting the prediction accuracy. In this regard, extensive trials were carried out to determine the optimum number of hidden neurons, defined

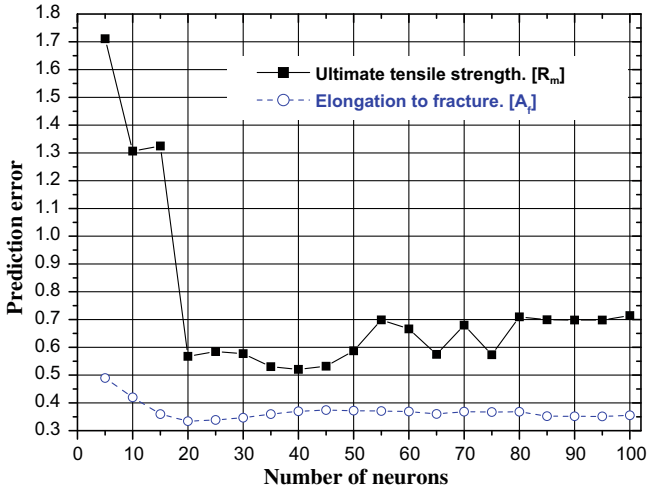


**Fig. 7.** Prediction error for different number of hidden neurons.

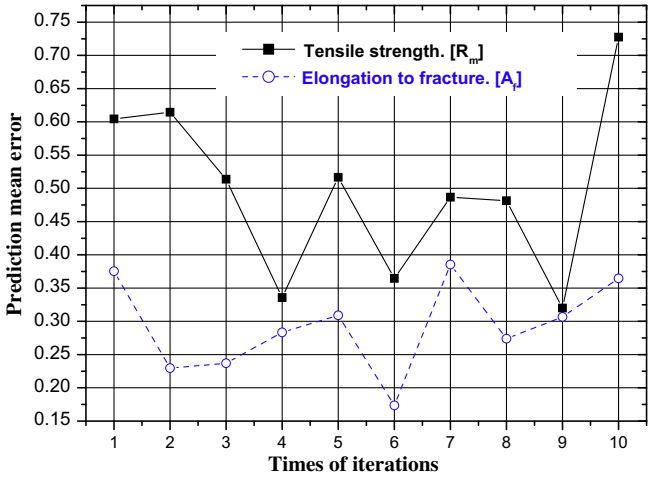


**Fig. 8.** Prediction mean error for different times of iterations, using the optimum number of hidden neurons.

by the RBF-NN structure where the best prediction accuracy is achieved. The prediction error, for different numbers of hidden neurons; i.e. from 5 to 100 neurons, using average pit depth and pitting density as input parameters, and ultimate tensile strength and elongation to fracture as output of the NN, is given in Fig. 7.

Greater RBF networks give higher accuracy in the estimation of the mechanical properties. The best prediction results were achieved, using 40 and 20 neurons for elongation of fracture and ultimate tensile strength, respectively. In order to confirm the stability of the method, the training and the prediction module were repeated 10 times, selecting randomly input/output pairs and using the optimum number of hidden neurons.

The analysis showed that the prediction accuracy is nearby constant for all iterations (Fig. 8). As it can be seen in this figure, the prediction accuracy ranges from 99.61% to 99.83% for the elongation to fracture and 99.27–99.68% for tensile strength, respectively. Displayed in Fig. 9a,b are the experimental results versus the NN results for tensile strength, and elongation to fracture.

As it can be seen in the following figures, there is a very good agreement between experimental and predicted values of the tensile strength. Similar correspondences were observed for the elongation to fracture.

To assess the significance of each of the input parameters, pit depth and pitting density, for the predicted ultimate tensile strength and tensile ductility to fracture, respectively, a parametric study has been realized. For this study, a new RBF-NN, with input parameter pit depth or pitting density, and output vector tensile strength and elongation to fracture, was designed.

The results obtained by the above analysis lead to the conclusion that the depth of corrosion attack (pit depth) has a stronger influence on the elongation to fracture (Fig. 10). On the contrary, the assessment of tensile strength is more accurate when pitting density has been used as input parameter. The fractographic analysis performed on the corroded tensile specimens, as discussed in Section 3.2 [18], show that the impact of pit depth on the decrease of the mechanical properties is stronger than that of pitting density.

## 6. Conclusions

A RBF-NN was used to assess the effect of existing corrosion damage on the residual tensile properties of structural magnesium alloy AZ31. An extensive experimental investigation including corrosion and mechanical tests as well as corrosion damage characteristics was carried out to train and validation the RBF-NN.

A set of only two parameters (pit depth and pitting density) is sufficient for robust correlation of existing corrosion damage to the mechanical properties of the corroded material.

The results show that the predicted values of the mechanical properties have been in very good agreement with the experimental data. The prediction accuracy achieved is encouraging for the

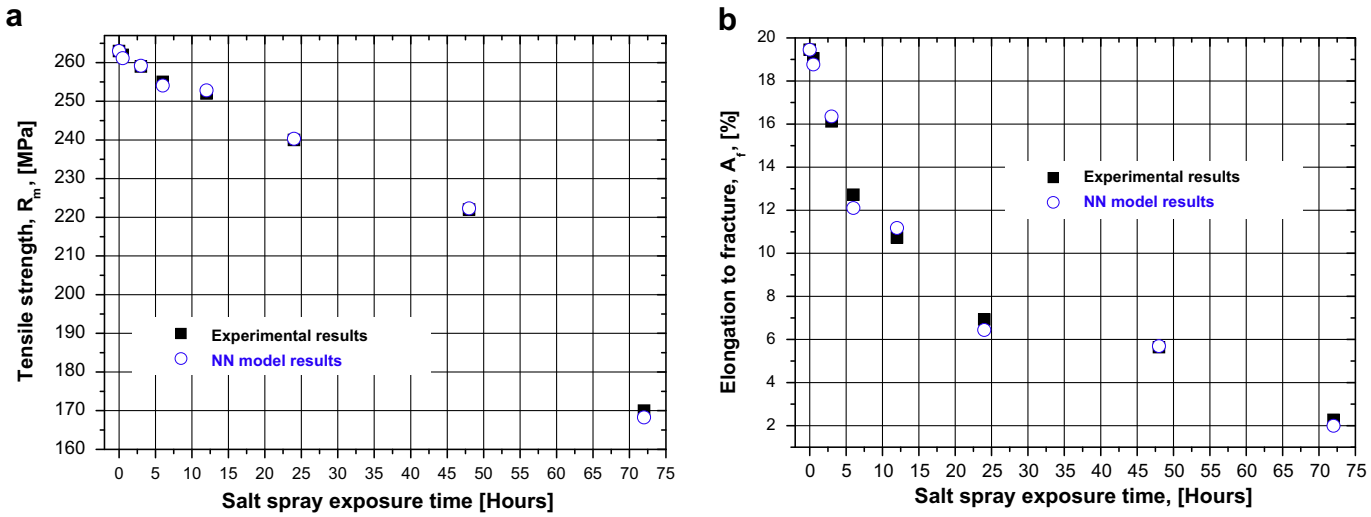


**Fig. 9.** Comparison of the experimental and NN results for (a) the tensile strength and for (b) the elongation to fracture.

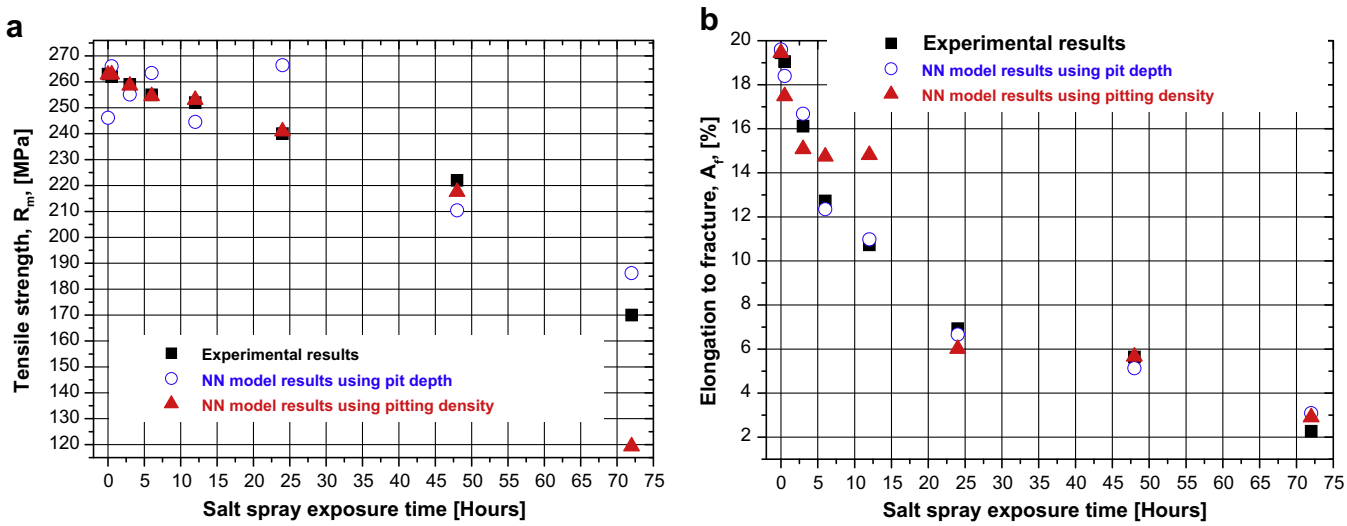


**Fig. 10.** Comparison of the experimental and NN results, using pit depth or pitting density, for (a) the tensile strength and for (b) the elongation to fracture.

exploitation of the developed model also for other alloys in use in engineering structural applications.

The NN analysis, which is consistent to fractographic analysis, shows that the pit depth has stronger effect on the decrease of the mechanical properties than that of pitting density.

Furthermore, reduction of time and cost for experimental procedures of materials and processes could be appreciably facilitated by exploiting the potential NN models.

## Acknowledgments

The authors are grateful to Prof. G.N. Haidemenopoulos and to Dr. E. Kamoutsi of University of Thessaly for performing SEM fractography. The experimental work performed in the present work is part of the AEROMAG Project "Aeronautical Application of Wrought Magnesium" (Project No. AST4-CT-2005-516152), which was supported by the European Union.

## References

[1] Benavides S. Corrosion in the aerospace industry, corrosion control in the aerospace industry. Woodhead Publishing Limited and CRC Press LLC; 2009. p. 1–14.
[2] Simpson DL, Brooks CL. Tailoring the structural integrity process to meet the challenges of aging aircraft. Int J Fatigue 1999;21:S1–S14.
[3] Pantelakis SpG, Kermanidis AT. Effect of corrosion on the mechanical behavior of aircraft aluminum alloys. Corrosion Control in the Aerospace Industry, Woodhead Publishing Limited and CRC Press LLC; 2009. p. 67–108.
[4] Calle LM. Corrosion control in space launch vehicles: corrosion control in the aerospace industry. Woodhead Publishing Limited and CRC Press LLC; 2009. p. 195–224.
[5] Petroyiannis PV, Kermanidis AlTh, Papanikos P, Pantelakis SpG. Corrosion-induced hydrogen embrittlement of 2024 and 6013 aluminum alloys. Theor Appl Fract Mech 2004;41:173–83.
[6] Kermanidis AlTh, Petroyiannis PV, Pantelakis SpG. Fatigue and damage tolerance of corroded 2024 T351 aircraft aluminum alloy. Theor Appl Fract Mech 2005;43:121–32.
[7] Pantelakis SpG, Alexopoulos ND, Chamos AN. Effect of salt spray corrosion on the tensile behaviour of wrought magnesium alloy AZ31. In: 7th International conference on magnesium alloys and their applications, Dresden, Germany; 2006.
[8] Apostolopoulos ChAlk, Papadopoulos MP, Pantelakis SpG. Tensile behavior of corroded reinforcing steel bars BSt 500s. Constr Build Mater 2006;20:782–9.
[9] Jones K, Shinde SR, Clark PN, Hoeppner DW. Effect of prior corrosion on short crack behavior in 2024-T3 aluminum alloy. Corros Sci 2008;50:2588–95.
[10] Song RG, Blawert C, Dietzel W, Atrens A. A study on stress corrosion cracking and hydrogen embrittlement of AZ31 magnesium alloy. Mater Sci Eng A 2005;399:308–17.
[11] Sterzovski Z, Nolan D, Carpenter KR, Dunne DP, Norrish J. Artificial neural networks for modelling the mechanical properties of steels in various applications. J Mater Process Technol 2005;170:536–44.
[12] Kusiak J, Kuziak R. Modelling of microstructure and mechanical properties of steel using the artificial neural network. J Mater Process Technol 2002;127:115–21.
[13] Bahrami A, Mousavi Anijdan SH, Ekrami A. Prediction of mechanical properties of DP steels using neural network model. J Alloys Compd 2005;392:177–82.
[14] Guo Z, Sha W. Modelling the correlation between processing parameters and properties of maraging steels using artificial neural network. Comput Mater Sci 2004;29:12–28.
[15] Huang CZ, Zhang L, He L, Sun J, Zou B, Li ZQ, et al. A study on the prediction of the mechanical properties of a ceramic tool based on an artificial neural network. J Mater Process Technol 2002;129:399–402.
[16] Malinov S, Sha W, McKeown JJ. Modeling the correlation between processing parameters and properties in titanium alloys using artificial neural network. Comput Mater Sci 2001;21:375–94.
[17] Pleune T, Chopra OK. Using artificial neural networks to predict the fatigue life of carbon and low-alloy steels. Nucl Eng Des 2000;197:1–12.
[18] Chamos AN. Mechanical behaviour of advanced aeronautical magnesium alloys. Doctoral Thesis, Department of Mechanical Engineering and Aeronautics, University of Patras, Greece; 2008.
[19] Haykin S. Neural networks: a comprehensive foundation. 2nd ed. New York: Prentice-Hall; 1999.